



Tracking control of an underwater manipulator using active disturbance rejection

Qirong Tang¹ · Daopeng Jin¹ · Rong Luo² · Rui Tao³ · Chonglun Li³ · Jiang Li¹ · Minghao Liu¹ · Chuan Wang⁴

Received: 4 September 2022 / Accepted: 15 August 2023 / Published online: 14 September 2023

© The Author(s), under exclusive licence to The Japan Society of Naval Architects and Ocean Engineers (JASNAOE) 2023

Abstract

An active disturbance rejection controller for a 2-DOF underwater manipulator is proposed in this study. The manipulator system has the characteristics of non-linearity, strong coupling and uncertainties within its model. Its operation is often disturbed by unknown water currents, so the anti-disturbance control of underwater manipulators has always been a challenge. The proposed controller in this study basically does not rely on the precise mathematical model of the object, and the model even can be decoupled. This method can eliminate the influence of model errors, time-varying parameters and external interference on the control effect. First, the entire manipulator treats different joints as several subsystems. For each joint subsystem, hydrodynamic forces, coupling terms between joints and unknown environmental disturbances are regarded as total disturbances. Subsequently, an extended state observer was designed to estimate and compensate for the total interference. In order to improve the disturbance observation effect of the extended state observer, the inertia matrix of the system is used to decouple the static part. Finally, the effectiveness of the proposed method is verified by both simulation and experiments. From the comparisons, it is confirmed that the quality of our controller in the presence of a certain inertial matrix error is better than traditional PD and continuous sliding mode control in terms of accuracy, dynamic characteristics as well as robustness.

Keywords Underwater manipulator · Active disturbance rejection controller · Trajectory tracking · Extended state observer · Uncertain systems

1 Introduction

In recent years, higher trajectory tracking accuracy is demanded in the field of robot and manipulator control. In many fields, such as astronomical observation [1], flight control [2], and underwater exploration [3, 4], in the presence of model uncertainties and unknown disturbances, the problem

of accurate trajectory tracking has attracted the attention of researchers.

Underwater manipulators are usually working in a complex hydraulic environment. Therefore, the model of underwater manipulator is more complicated than that of common manipulators because of the unknown water flow disturbances, additional viscous resistance of fluid and additional

✉ Qirong Tang
qirong.tang@outlook.com

Daopeng Jin
17853142827@163.com

Rong Luo
luorong583@163.com

Rui Tao
48071646@qq.com

Chonglun Li
512718156@qq.com

Jiang Li
lixutong@tongji.edu.cn

Minghao Liu
2130213@tongji.edu.cn

Chuan Wang
hg04381@163.com

¹ Laboratory of Robotics and Multibody System, Tongji University, Shanghai 201804, China

² Naval Research Academy, Beijing 102442, China

³ Naval Research Institute, Shanghai 200235, People's Republic of China

⁴ Naval Medical Center, Shanghai 200433, People's Republic of China

mass forces [5]. The nonlinear and uncertain system, coupled with multiple external disturbances in the underwater environment, have become principal challenges for conventional control strategies.

The control methods of the underwater manipulator system are not limited to PID control [6, 7], adaptive control [8], neural network control [9, 10] and sliding mode control [11]. For the multi-DOF underwater manipulator, a controller containing model parameter estimation and multi-layer closed-loop PID is designed [12], but nonlinear disturbances are not compensated. An adaptive control robot algorithm was proposed by Tomeiet al., which combined PD controller and dynamic compensation model [13], it enhances the nonlinear control accuracy, but requires a more accurate dynamic model of the manipulator. Neural network control [14] does not depend on the exact mathematical model, but its sample data for training is a key issue. Sliding mode control is extensively used in anti-jamming and indeterminate models. Bin Xu et al. designed an improved sliding mode controller based on fuzzy logic [15], but the output torque of the controller yet had the problem of jitter.

Since these traditional control strategies are modeled to perform in a specified and known “real” environment and cannot accommodate unavoidable disturbances, they cannot perform well enough in the presence of some modeling uncertainties. Therefore, the problem of disturbance rejection has become the main research focus in the field of underwater manipulator control. Aiming at the limitations of PID control, The Active Disturbance Rejection Controller (ADRC) [16] was provided. Based on the traditional PID control, new nonlinear dynamic structures are proposed: extended state observer (ESO), tracking differentiator (TD) [17] and nonlinear state error feedback (NLSEF) [18]. This disturbance observer method has caused great research interest, and is regarded as the inheritance and improvement of traditional PID controllers, and many comparisons have been performed to prove ADRC’s superiority [19]. The ADRC aims to not only estimate the state of the system, but also estimate most of the unknown concentrated interference [20]. On the basis of the ADRC method, the total disturbance can be considered an additional state variable in the system, estimated by a linear state observer, and finally compensated in the feedback signal. MahMoud et al. applied the ADRC to the trajectory tracking of a two-link manipulator and the simulation showed that it had better anti-jamming capability than PID [21]. Radosław used the Lyapunov analysis to prove the stability of ADRC in manipulator control and proposed model low-order estimation compensation to further improve its stability [22]. Therefore, the goal of this research is to verify actual quality of ADRC approach in controlling a complex MIMO systems without a precise model. This study takes the advantage of the ADRC to control an underwater manipulator with two rotational joints. Uncertain part

of the model, the coupling term between joints and unsure environmental disturbances are considered to be the total disturbance. Therefore, the extended state observer is built to estimate them, and then feedback control law is used to actively compensate them.

The remaining parts of this paper are organized as follows: Sect. 2 presents the system overview of the underwater manipulator. Section 3 recalls basic components behind the ADRC method and focuses on the extended state observer. ADRC decoupling design of underwater manipulator is presented in Sect. 4. Then, the simulation is divided into two cases: system with inertia matrix error and system with external disturbances, which is presented in Sect. 5. Experiments are performed in Sect. 6, while the proposed method’s effectiveness is proven. Finally, Sect. 7 concludes this paper.

2 System overview

The system mainly includes a 2-DOF underwater manipulator. As shown in Fig. 1, it can be simplified as a dual-link system, whose two links can be represented by M_1 and M_2 , respectively. The end of the manipulator is equipped with an end effector, which have the final effect of performing some certain underwater tasks. In this study, ADRC is used to control the manipulator to realize the tracking control of the desired trajectory in the joint space. The Cartesian coordinate system of underwater manipulator is shown in Fig. 1, which consists of the reference fixed coordinate system $O - x_0y_0z_0$, the joint coordinate system $O_i - x_iy_iz_i (i = 1, 2)$ and the end-effector coordinate system $O_3 - x_3y_3z_3$. Here O is the origin of the reference fixed coordinate system, and O_1, O_2 are the rotation centers of the robot arms M_1, M_2 . Here q_1 is the angle between the x_1 axis and the x_0 axis, while q_2 is the angle between the x_2 axis and the x_1 axis, $l_i (i = 1, 2)$ is the length of the arms. Assuming that each link

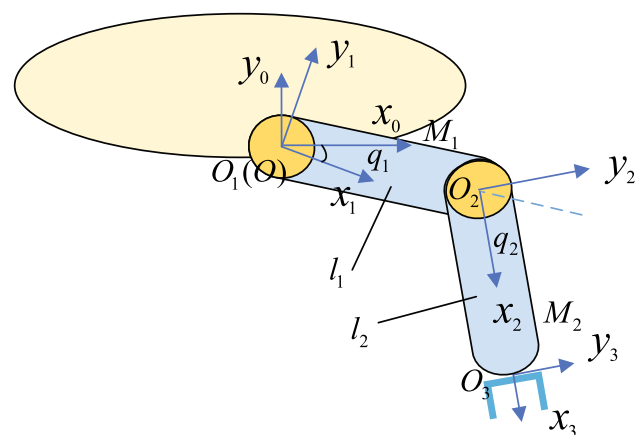


Fig. 1 A 2-DOF underwater manipulator model

of the manipulator is a homogeneous element, the center of the link and the center of gravity are coincident. And assuming that the underwater vehicle is very large relative to the underwater manipulator, so that the swing of the end effector can be ignored. Based on the Lagrangian energy equation, the dynamic model of underwater manipulator is given as follows:

$$\tau + w(t) = M(q)\ddot{q} + C(q, \dot{q})\dot{q} + D(q, \dot{q})\dot{q} + G(q), \quad (1)$$

where $M(q) \in \mathbb{R}^{2 \times 2}$ is the inertia matrix, $C(q, \dot{q}) \in \mathbb{R}^{2 \times 2}$ is the centrifugal and Coriolis vector, $D(q, \dot{q})$ is the hydrodynamic damping matrix formed by the terms due to fluid viscous resistance and additional mass force, and $G(q) \in \mathbb{R}^{2 \times 1}$ is the gravity vector which considered the buoyant force, q, \dot{q} and \ddot{q} are joint position, joint velocity and joint acceleration vectors, respectively. The $\tau \in \mathbb{R}^{2 \times 1}$ is a joint input torque vector. Since this study focus on the practical performance of the underwater manipulator, $w(t)$ is adopted to represent the unknown disturbance including the unknown fluid disturbance and model uncertainty such as friction of the joints. and $w(t)$ is an unknown disturbance caused by complex fluid flow.

3 ADRC method

3.1 Basic components

The active disturbance rejection controller (ADRC) depends on the role of the disturbance rejection, which is the main processor of the controller. It regards the unknown dynamics and external disturbances in the system as the total disturbance of the controlled object and takes it as the expanded state variable. The expanded state observer (ESO) estimates the total disturbance and takes the initiative compensation and cancellation. So the system with non-linearity and unknown disturbance is restored to a simple integral series type to realize active disturbance rejection. The principle block diagram of basic ADRC for a typical single-input

single-output (SISO) second-order system is shown in Fig. 2. It is mainly composed of tracking differentiator (TD), extended state observer (ESO), nonlinear states error feedback control laws (NLSEF) and disturbance compensation. The TD realizes the preprocessing of the given tracking signal v to make the change process more reasonable, and obtains the transition process v_1 and its derivative signal v_2 that filter noise and retain the original signal characteristics. The idea of ESO estimates the state quantity and the total disturbance of the system in real time, and the NLSEF is a nonlinear PID algorithm to ensure that the output of the system can effectively track the given signal.

3.2 Extended state observer

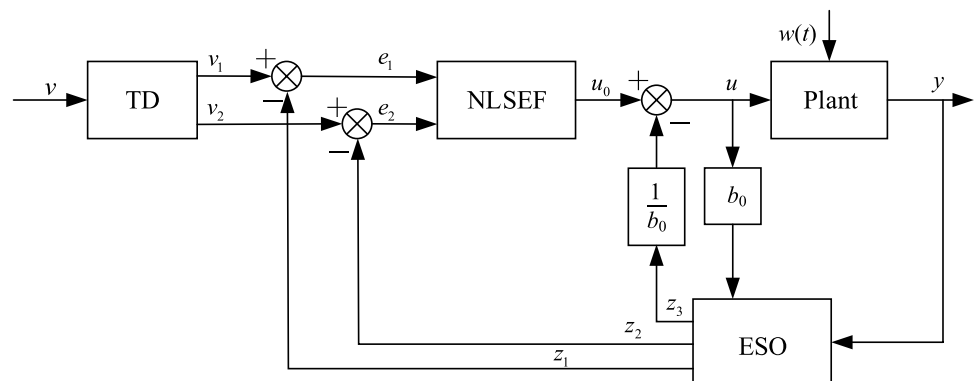
The performance of ADRC mainly depends on the extended state observer (ESO). The ESO estimates the state of the object and the total perturbation acting on the object based on the output and input signals. It often aims at a second-order system with single-input and single-output, which is expressed by

$$\begin{cases} \ddot{x} = f(x, \dot{x}, w, t) + bu \\ y = x \end{cases}, \quad (2)$$

where x is the system state variable, u is the system input, b is the input control matrix, y is the system output signal, w represents the overall external disturbances, and f is defined as the total disturbance of the system, which is a nonlinear function, which contains all internal disturbances, external disturbances and the system nonlinear terms. In order to realize the estimation and compensation of f , ADRC defines it as an extended state value x_3 of the system. Thereby, the above system can be formulated using the assumed phase state variables as

$$\begin{cases} \dot{x}_1 = x_2 \\ \dot{x}_2 = x_3 + bu \\ \dot{x}_3 = \dot{f} \end{cases}. \quad (3)$$

Fig. 2 The structure of a basic ADRC scheme for a second-order system



Design a nonlinear extended state observer for the second-order system, one has

$$\begin{cases} e = z_1 - y \\ \dot{z}_1 = z_2 - \beta_1 fal(e, \alpha_1, \delta) \\ \dot{z}_2 = z_3 - \beta_2 fal(e, \alpha_2, \delta) + b_0 u \\ \dot{z}_3 = -\beta_3 fal(e, \alpha_3, \delta) \end{cases} \quad (4)$$

where z_1, z_2 and z_3 are the observed values of the state variables, where z_3 is the observed value of the system’s total disturbance x_3 (expanded state quantity), $\beta_i (i = 1, 2, 3)$ is the observer parameter, b_0 is an estimation of parameter b , and fal is a continuous power function with a linear segment near the origin, which is defined as

$$fal(e, \alpha, \delta) = \begin{cases} \frac{e}{(\delta^{1-\alpha})} & |e| \leq \delta \\ |e|^\alpha \text{sgn}(e) & |e| > \delta \end{cases}, \quad (5)$$

where δ is the length of the linear segment, α is an adjustable parameter to be designed. The specific values of α in Eq. 4 are α_1, α_2 and α_3 which are usually set as 1, 0.5 and 0.25, respectively. Finally, ESO achieves a high accuracy for the estimation of the state variables of the system, i.e., Eq. 2, including the expanded state quantity of the total disturbance. In Eq. 4, the input control parameter is approximated as a constant b_0 , then the ESO estimates the unknown part of the system input $(b - b_0)u$ as the part of total disturbance:

$$\begin{cases} z_1 \rightarrow x_1 \\ z_2 \rightarrow x_2 \\ z_3 \rightarrow x_3 = f(x_1, x_2, w, t) + (b - b_0)u \end{cases}. \quad (6)$$

4 ADRC decoupling design for 2-DOF underwater manipulator

In this case, the ADRC control method is used on a 2-DOF underwater manipulator, a second-order system which is described by Eq. 1. This controlled object is a Multi-Input-Multi-Output (MIMO) system, and one regards each joint of the manipulator as a Single-Input-Single-Output (SISO) system. There is a coupling between the two joints of the underwater manipulator, and the movement of one joint will affect the motion of another one, and at the same time appear strong non-linearity. This part can be regarded as internal disturbance of the system, which is part of the item f . For the 2-DOF underwater manipulator, the ADRC is designed for the two joints separately. The ADRC for the 2-DOF manipulator is decoupled in the following way shown in Fig. 3. The concepts used in the mentioned decoupling scheme are shown below as well.

4.1 Tracking differentiator

For the real angle position of the i -th joint qd_i and its given reference position, the transition process can be configured by TD through its tracking signal v_{i1} and differential v_{i2} . The linear TD is constructed as follows:

$$\begin{cases} FH = -r(v_{i1} - qd_i) - 2r \\ v_{i1} = v_{i1} + hv_{i2} \\ v_{i2} = v_{i2} + hFH \end{cases}, \quad (7)$$

where $h = 0.01s$ represents the step size of discretization, r respects the coefficient of tracking speed and FH is a linear function which is self-defined.

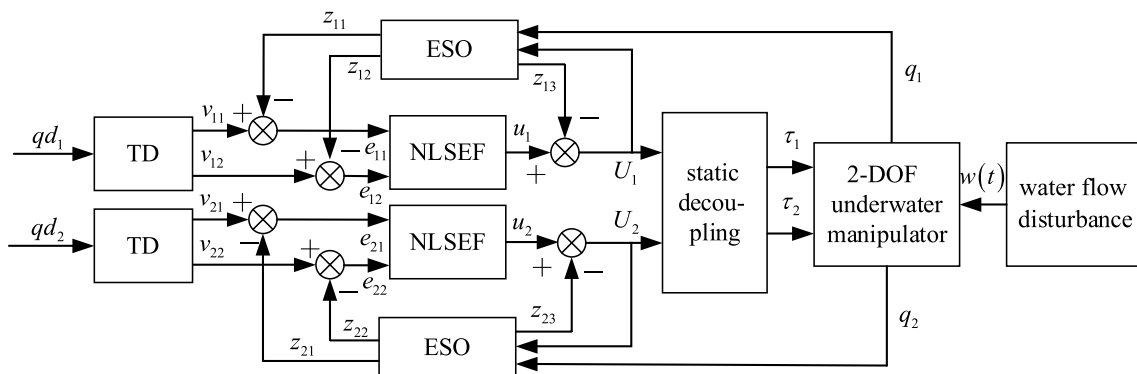


Fig. 3 An ADRC decoupling scheme for the 2-DOF underwater manipulator

4.2 Extended state observer

The 2-DOF underwater manipulator's dynamic model, i.e., Eq. 1, can be converted to the following form:

$$\ddot{\mathbf{q}} = \left[\dot{q}_1 \quad \dot{q}_2 \right]^T = \underbrace{\mathbf{M}^{-1}(\mathbf{w}(t) - \mathbf{C}\dot{\mathbf{q}} - \mathbf{D}\dot{\mathbf{q}} - \mathbf{G})}_{f(\mathbf{q}, \dot{\mathbf{q}}, \mathbf{w}(t), t)} + \underbrace{\mathbf{M}^{-1}}_b \left[\tau_1 \quad \tau_2 \right]^T, \quad (8)$$

where $\mathbf{w}(t)$ is the disturbance of the flow, $f(\mathbf{q}, \dot{\mathbf{q}}, \mathbf{w}(t), t)$ is the unknown part of the system, which is time-varying and include the system uncertainty, internal disturbances caused by the coupling between joints, and external fluid flow disturbance as well. If each joint of the underwater manipulator is treated as an SISO second-order independent system, $\mathbf{M}^{-1}(\mathbf{w}(t) - \mathbf{C}\dot{\mathbf{q}} - \mathbf{D}\dot{\mathbf{q}} - \mathbf{G})$ is the system dynamics coupling term while $\mathbf{M}^{-1} \left[\tau_1 \quad \tau_2 \right]^T$ is the static coupling term. Defining the virtual control input $\left[U_1 \quad U_2 \right] = \mathbf{M}^{-1} \left[\tau_1 \quad \tau_2 \right]^T$ using inertia matrix \mathbf{M} , the static coupling part can be decoupled, and the state space of the i -th ($i = 1, 2$) joint can be obtained

$$\begin{cases} \ddot{q}_i = f(\mathbf{q}, \dot{\mathbf{q}}, w_i(t), t) + U_i \\ y_i = q_i \end{cases} \quad (9)$$

For the control object in this case, state x_{i1} corresponds to the joint angle value q_i of the i -th joint of the manipulator, and state x_{i2} corresponds to the angle velocity value \dot{q}_i . The U_i above is the virtual torque acting on the i -th joint, $w_i(t)$ is the disturbance from the external environment, the nonlinear function f represents the total disturbance acting on the underwater manipulator which contains the internal and external disturbance and nonlinear terms. Aiming to estimate and eliminate the influence of the total disturbance f , one defined f as a state x_{i3} of ADRC system which is shown as follows:

$$x_{i3} = f(\mathbf{q}, \dot{\mathbf{q}}, w_i(t), t). \quad (10)$$

Then, the ESO is designed for each joint of the manipulator independently are as follows:

$$\begin{cases} e_i = z_{i1} - q_i \\ \dot{z}_{i1} = z_{i2} - \beta_{i1}fal(e, \alpha_{i1}, \delta_i) \\ \dot{z}_{i2} = z_{i3} - \beta_{i2}fal(e, \alpha_{i2}, \delta_i) + U_i \\ \dot{z}_{i3} = -\beta_{i3}fal(e, \alpha_{i3}, \delta_i) \end{cases}, \quad (11)$$

where z_{i1} , z_{i2} and z_{i3} are the estimation of i -th joint states. Using ESO to estimate the state variables of the system, including the total disturbance Eq. 6:

$$\begin{cases} z_{i1} \rightarrow q_i \\ z_{i2} \rightarrow \dot{q}_i \\ z_{i3} \rightarrow x_{i3} = f(\mathbf{q}, \dot{\mathbf{q}}, w_i(t), t) \end{cases}. \quad (12)$$

The estimation value of joint state z_{i1} , z_{i2} is inputted into the state feedback control law, while z_{i3} is used to compensate the control torque which are shown as follows:

$$U_i = u_i - z_{i3}. \quad (13)$$

Combining Eqs. 9, 11 and 13, each joint of the manipulator is compensated by ESO and taken as a linear integral series system, both with constant input amplification factor joints of value 1. Afterwards, the virtual control torque \mathbf{U} which is defined by Eq. 9 can be converted to driving torque $\boldsymbol{\tau}$ of the joints by the static decoupling law $\left[\tau_1 \quad \tau_2 \right]^T = \mathbf{M} \left[U_1 \quad U_2 \right]^T$.

4.3 Nonlinear state error feedback control law

The NLSEF is a nonlinear control combination, instead of the linear combination of the traditional PID controller, which can obtain a more effective error feedback control rate. It integrates the nonlinear function $fhan(e_1, ce_2, r_1, h_1)$, which sometimes performs much better than the linear control [18]. For the i -th junction, the NLSEF is constructed by the following equations:

$$\begin{cases} e_{i1} = v_{i1} - z_{i1} \\ e_{i2} = v_{i2} - z_{i2} \\ u_i = -fhan(e_{i1}, ce_{i2}, r_1, h_1) \end{cases}, \quad (14)$$

$$\begin{cases} d = r_1 h_1^2, a_0 = h_1 c e_2, y = e_1 + a_0, a_1 = \sqrt{d(d + 8|y|)} \\ a_2 = a_0 + \frac{(a_1 - d)}{2} \operatorname{sgn}(y) \\ a = (a_0 + y - a_2) \frac{\operatorname{sgn}(y + d) - \operatorname{sgn}(y - d)}{2} + a_2 \\ fhan = \\ -r_1 \left[\frac{a}{d} - \operatorname{sgn}(a) \right] \frac{\operatorname{sgn}(a + d) - \operatorname{sgn}(a - d)}{2} - r_0 \operatorname{sgn}(a) \end{cases}. \quad (15)$$

Here e_{i1} is the joint angle position error, e_{i2} is the joint angle velocity error, c is the damping coefficient, r_1 is a convergence coefficient, h_1 is the factor of precision and u_i is the output of the control law. And $fhan$ is an optimal control synthesis function derived from discrete optimization theory,

Table 1 Basic physical parameters

Items	Link M_1	Link M_2
m/kg	2.38	1.96
l/m	0.32	0.32
$I_{zz}/\text{kg} \cdot \text{m}^2$	0.0198	0.0168

Table 2 D-H parameters

i	$\alpha_{i-1}(\text{rad})$	$a_{i-1}(\text{m})$	$d_i(\text{m})$	$\theta_i(\text{rad})$
1	0	0	0	q_1
2	0	0.32	0	q_2
3	0	0.32	0	0

which is defined in [18]. After the compensation of the total disturbance by ESO and the decoupling by static decoupling method, and applying the obtained control torque input to the joint subsystem, then it is concerted to

$$\begin{bmatrix} \tau_1 \\ \tau_2 \end{bmatrix} = \mathbf{M} \begin{bmatrix} -fhan(e_{11}, ce_{12}, r_1, h_1) - z_{13} \\ -fhan(e_{21}, ce_{22}, r_1, h_1) - z_{23} \end{bmatrix}. \tag{16}$$

5 Simulations

The simulation object 2-DOF underwater manipulator is shown in Fig. 1. The physical parameters, D-H parameters of the underwater manipulator are listed in Tables 1 and 2. The ADRC parameters is shown in Table 3. The aim of simulations is to verify the performance of ADRC method without the precise modeling, and simulations has two part. For the first case, simulation tests the influence level of model uncertainty on ADRC control quality. For the second case, simulation shows tracking performance of the underwater manipulator with proposed controller. The three control methods track the same desired trajectory in two cases, which the trajectory is designed as

$$\begin{cases} qd_1 = \frac{\pi}{4} + \frac{\pi}{4} \sin\left(0.5t + \frac{\pi}{4}\right) \\ qd_2 = \frac{\pi}{6} \sin\left(0.8t + \frac{\pi}{4}\right) \end{cases}. \tag{17}$$

Table 3 ADRC parameters

Joint	TD		ESO				NLSEF		
	h	r	β_1	β_2	β_3	δ	r_1	h_1	c
1	0.01	10	2000	1290	1200	0.03	100	0.01	2.7
2	0.01	10	2000	1936	780	0.03	100	0.01	1.3

5.1 System with inertia matrix error

In the first part, ADRC is applied for the underwater manipulator in the view of nonlinear system. The inertia matrix \mathbf{M} is very important to transform its static decoupling into several joint subsystems. Considering the control quality with the presence of model uncertainty. In the simulation, one adds a variation range to the inertia matrix \mathbf{M} in Eq. 1 as the model error, but does not impose additional external disturbances.

In the upcoming experiments, we set different inertial matrix errors in the trajectory tracking task. It is desired that the actual angular position tracking error of each joint are under different inertial matrix errors. A parameter ρ is used to characterize the error between the inertial matrix \mathbf{M}_{sdl} during static decoupling ($[\tau_1 \ \tau_2]^T = \mathbf{M}_{sdl} [U_1 \ U_2]^T$) and real inertial matrix \mathbf{M}_{rea} of the underwater manipulator, which is defined as

$$\mathbf{M}_{sdl} = \rho \mathbf{M}_{rea}. \tag{18}$$

In the simulation, it sets $\rho = 1, 0.7,$ and $1.3,$ respectively, to verify the basic tracking control quality of the ADRC. The comparisons of the trajectory tracking error for the system with different inertia matrix errors are presented in Fig. 4. No significant different can be seen here, for three different values of ρ . The ADRC technique can realize good quality of angle tracking and angular velocity tracking. At the first 3 s of the simulation, there is a transition process that the tracking error is rapidly reduced to 0. After that, the tracking error has been kept at a small value near 0. Therefore, the ADRC can guarantee that the angle position error is at the range of $\pm 0.01\text{rad}$, and the angular velocity error is at the range of $\pm 0.02\text{rad/s}$. However, In the case of $\rho = 0$ (that means $\mathbf{M}_{sdl} = \mathbf{M}_{rea}$), the ADRC seems to be more efficient, the early transition process is shorter and the overshoot is smaller. In Fig. 4d, when $\rho = 1, 0.7$ or $\rho = 1.3,$ respectively, a small oscillation process appeared at the 1.3 second, but it quickly adjusted and disappeared.

5.2 System with external disturbances

In the second part, this study uses the original underwater manipulator as a simulation prototype ($\rho = 0$). The parameters of the mathematical model are constant and remain unchanged but subject to external disturbances. Therefore, to verify control quality of ADRC, a PD controller

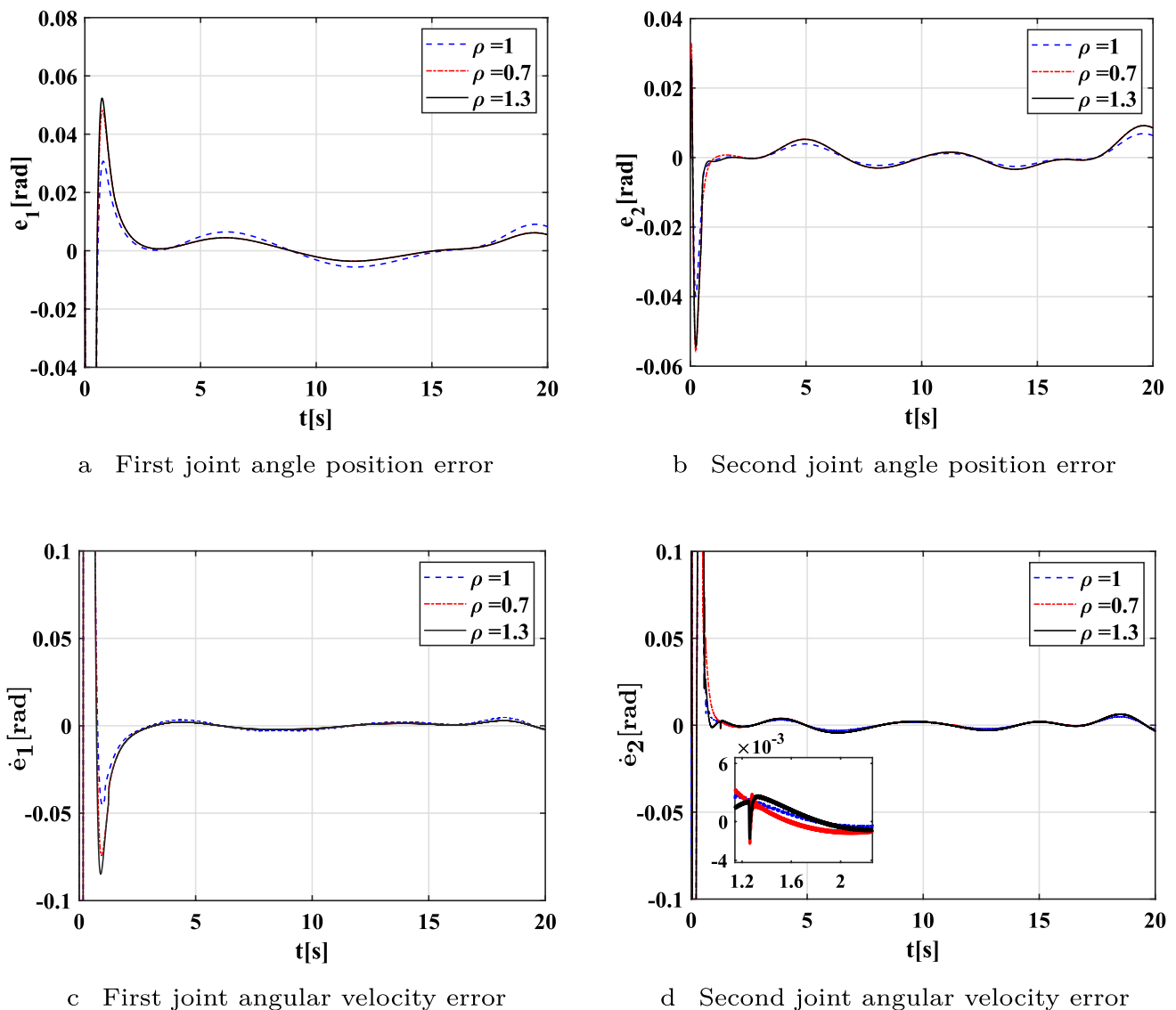


Fig. 4 Trajectory tracking error e for the system with different inertia matrix errors

and a (continuous sliding mode controller) CSMC were chosen to compared with ADRC with sudden external disturbances while eliminating the influence of changes in internal model parameters. Here the PD controller is chosen instead of a PID controller is because that the PD controller, with its faster response to external influences, is better suited for application in practical underwater environments.

Based on the original underwater manipulator as a simulation prototype, the entire simulation process also spends 20 s. Since the expected trajectory is often designed to be relatively smooth in practical tasks, so a

sine wave trajectory is adopted as the tracking trajectory. The applied external disturbance value is 0 until 10s. At the 10s, external disturbances are added to the underwater manipulator, which is defined as follows:

$$\begin{cases} w_1 = 5 + 15 \sin\left(0.5t - \frac{\pi}{4}\right) \\ w_2 = 5 + 2 \sin\left(0.5t + \frac{\pi}{6}\right) \end{cases} \quad (19)$$

Figure 5 depicts the results of the signal tracking simulator. It shows that under the condition of without external

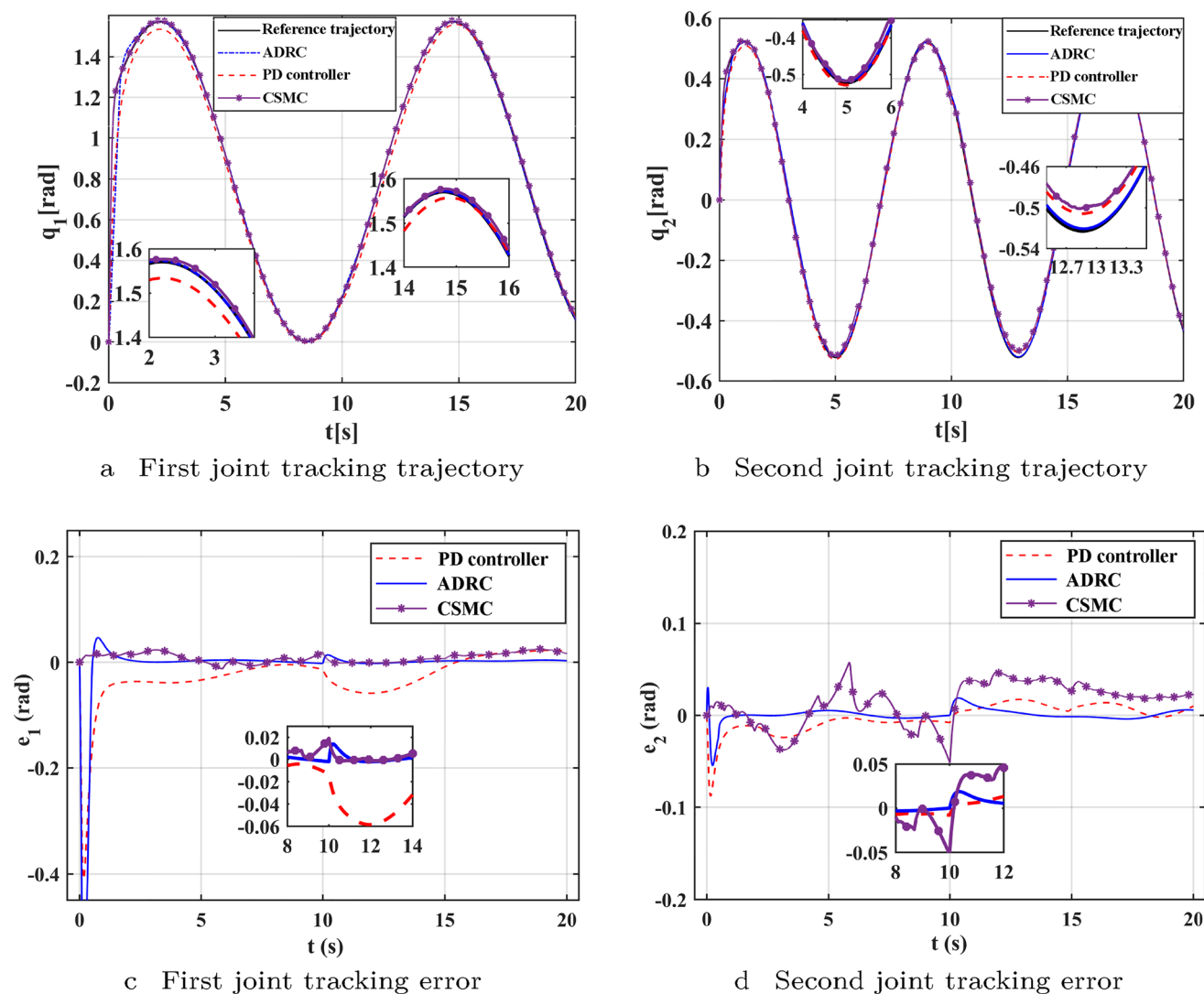


Fig. 5 Joint angle signal tracking results for the system with external disturbances

disturbance in the first 10 s, and with external disturbance in the second 10 s. Compared with PD controller and CSMC, the proposed ADRC has better performance under different conditions. Fig. 6 also shows the results of the joint input torque of three tracking controllers. From the results of the chattering problem, we can know the proposed ADRC obviously has good dynamic performance.

Considering the various types of disturbances that may occur in underwater environments, including disturbances from the underwater environment and disturbances caused by the robot itself, we added noise to the applied disturbance signals (noise power of 0.5 on link 1 and noise power of 0.1 on link 2), which is shown in Fig. 7. It can be seen that ADRC can control the underwater manipulator to

track the desired trajectory with minimal errors when facing with external disturbance with high uncertainty. This demonstrates the robustness of ADRC against external disturbances.

In order to simulate the performance of the proposed method in underwater tasks, a target point is predefined in the task space of the underwater manipulator to plan a trajectory using RRT for end actuator. After converting the end actuator trajectory into joint trajectory, the manipulator is tested in simulation, and the tracking performance and the input of ADRC are shown in Fig. 8a, b. It can be seen that under the control of ADRC, the underwater manipulator tracks the reference trajectory with small errors.

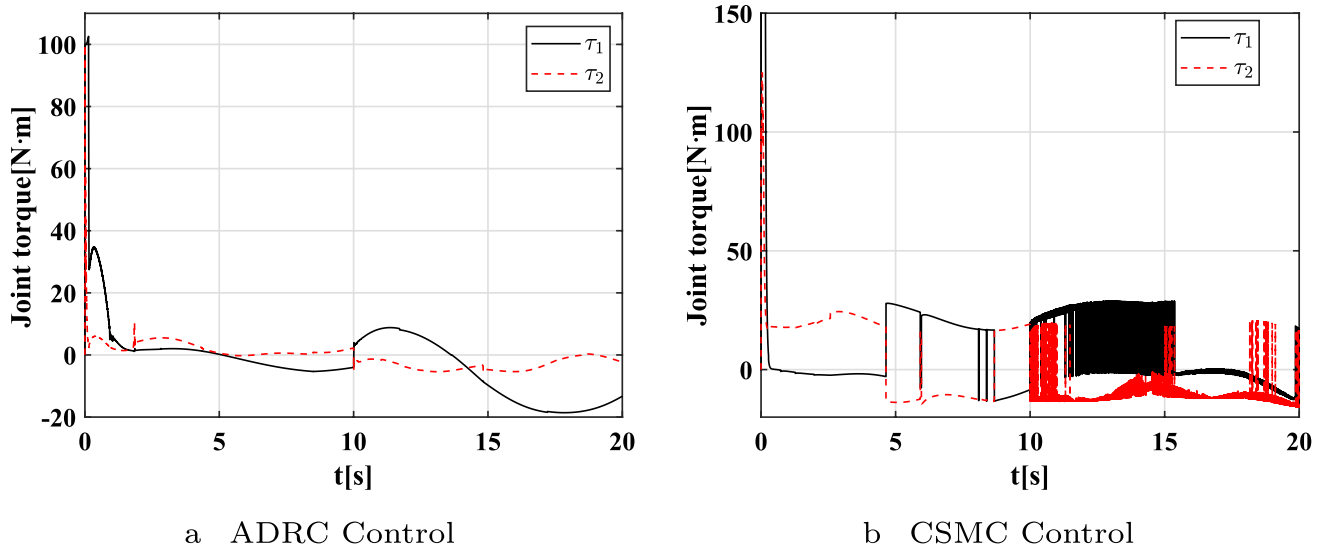


Fig. 6 Joint input torque results of ADRC and CSMC

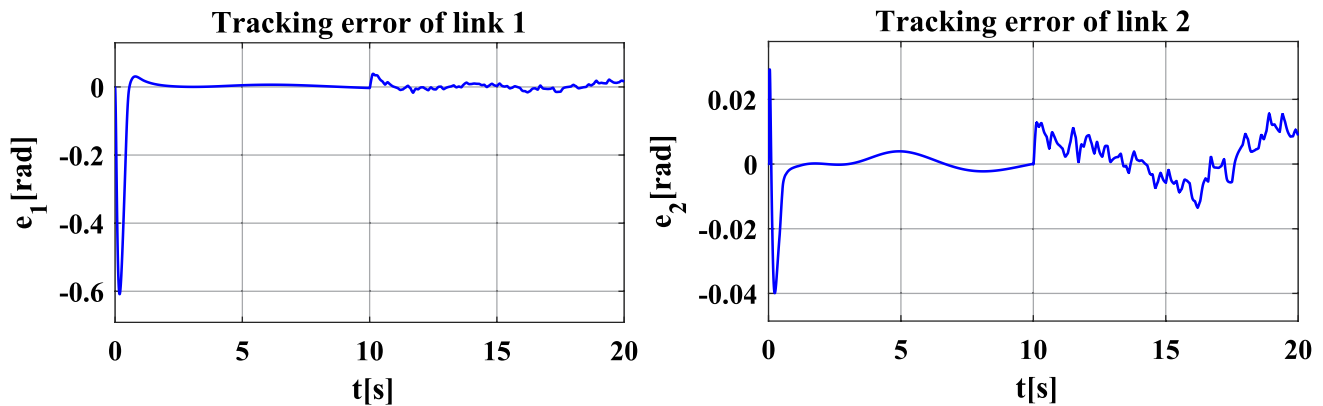


Fig. 7 Tracking error of two links with disturbances with noise

6 Experiments

The proposed method of this study is applied to the actual underwater manipulator in the pool.

6.1 Experimental configuration

The trajectory tracking experimental platform consists of a round experimental pool, a Speedgoat real-time target simulator, a robotic mounting bracket, and 2-DOF underwater manipulator is shown as Fig. 9. Considering the current experimental conditions, the artificial wave is used to simulate the water flow disturbance during the operation of the actual underwater manipulator, which is shown in Fig. 10.

And the influence caused by waves on the manipulator can be approximated by a sine wave [23]. The effective wave height of the artificial wave is proposed to be 0.1 m. The peak frequency does not exceed 0.5 Hz. The underwater manipulator is fixed to a aluminum alloy shelf and the center of the first joint of the underwater manipulator is flush with the water surface. The main function of Speedgoat real-time target simulator is to realize the real-time mapping conversion from the MATLAB/Simulink simulation program on the host computer to the control signal of the electronic control system of the underwater manipulator. Speedgoat real-time target machine supports a variety of protocol interfaces, including CAN, RS232, RS422, RS485, Ethernet, etc., and can be further installed with expansion boards to achieve more features.

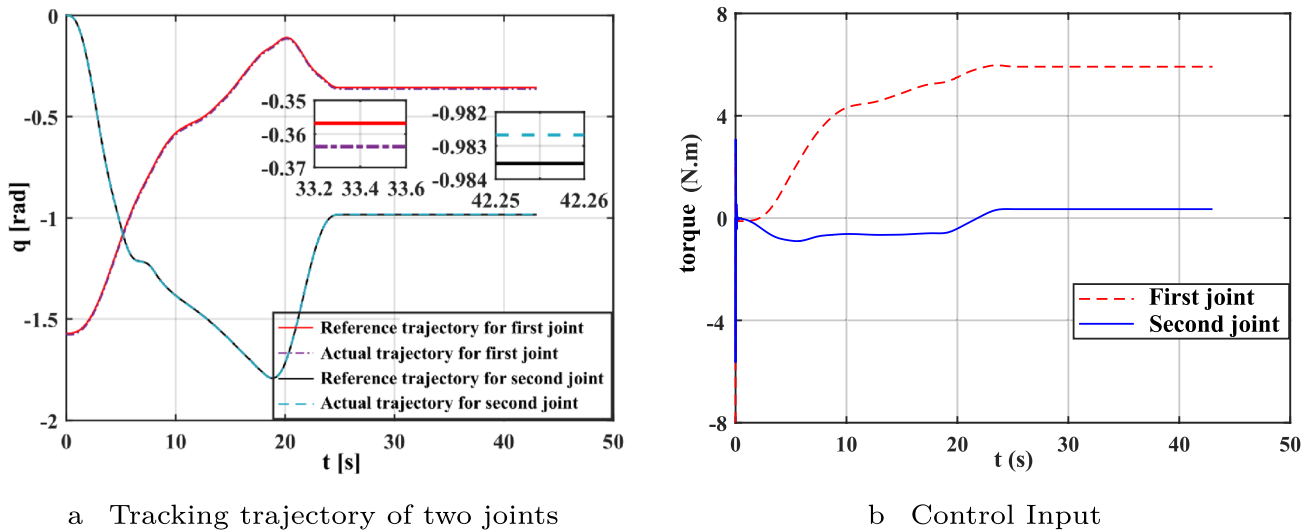


Fig. 8 Tracking trajectory and control input using ADRC

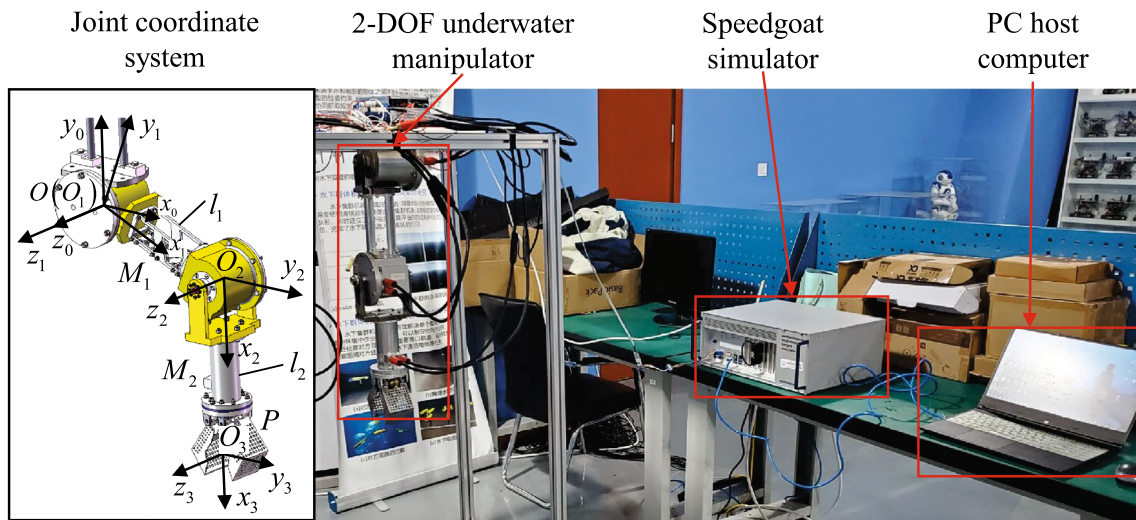


Fig. 9 Underwater manipulator trajectory tracking experimental platform



Fig. 10 Experimental round pool. The diameter of the round pool is 5 m and the depth is 1.5 m

6.2 Experimental architecture

The Speedgoat real-time target simulator is the bridge between the PC host computer and manipulator, which specifically completes the issuance of joint motor control commands and the return of the actual motor angle sensor data. As shown in Fig. 11, the control architecture of the underwater dual-arm system experimental platform designed in this study.

The MATLAB/Simulink Real-Time simulation program is executed on a PC host computer with the core of AMD R7 5800H 4.4 GHz and the RAM of 32G, which performs

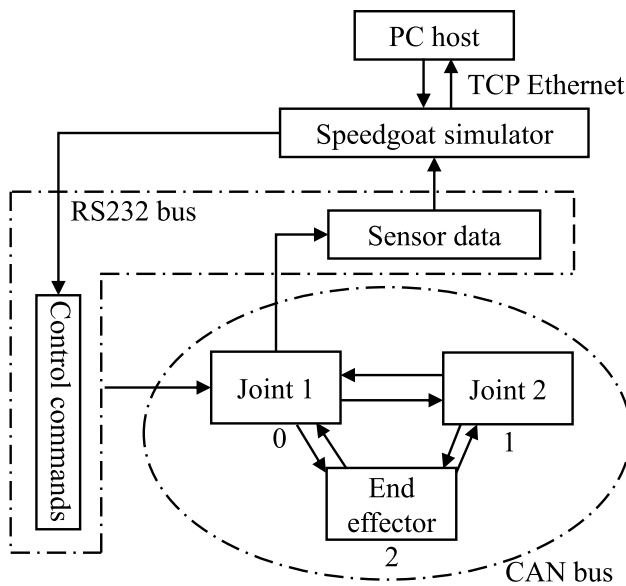


Fig. 11 Experimental platform control architecture diagram

fixed-step discretization processing, and realizes the connection with the Speedgoat real-time target computer through Ethernet. Then, the Speedgoat real-time target simulator translates the MATLAB program into an executable file and outputs control, which is received by the manipulator through the RS232 bus (9600 bps). To precisely respond to the input torque of each joint, FHA-14C-100 and FHA-11C-100 motors with high level of torque performance are adopted for the manipulator. Therefore, the underwater manipulator links all joints into the same CAN control network. In the entire control architecture, the Speedgoat real-time target simulator and the PC host computer maintain real-time synchronization, which is determined by the underlying hardware. In the meanwhile, the control instructions of each motor of the manipulator system is also in accordance with the synchronization principle programming. Therefore, the step size of the upper and lower layers of the entire control architecture is consistent.

6.3 Parameters setting

The whole experiment lasted 43 s, and the control frequency of the controller is 0.05 s. This control period is chosen for the aim of demonstrating the performance of the controller that is not rely on fast control period. This enables testing whether the proposed method can be applied to general underwater manipulators. In order to comparing and verifying the greater performance of the ADRC decoupling controller for the dual-joint underwater manipulator proposed, the PD feedback linearization controller and CSMC are also set, respectively. The actual ADRC parameter are also show in Table 3.

6.4 Result analysis

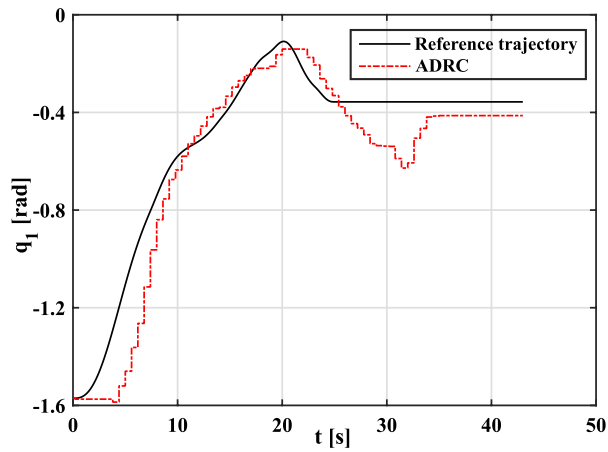
In the entire trajectory tracking experiment, the Speedgoat target simulator recorded each joint angular position of the underwater manipulator in real time. After the noise reduction process, the actual angle of each joint is shown in Fig. 12. At the same time, Table 4 shows the tracking error with difference controllers.

According to the analysis of Fig. 12a–f, compared with the feedback linearized PD controller and CSMC, the proposed method in this study has the best control performance. In the first 24 s, the adjustment time of the ADRC is shorter, and the tracking error is rapidly reduced. While the feedback linearized PD control and CSMC control both have a large overshoot. For the following 18 s, the feedback linearized PD control has a large oscillation especially in Fig. 12e, which is mainly caused by the overshoot of PD controller. Meanwhile, the CSMC control has a long adjustment time and has a large motion steady-state error as well as chattering phenomenon, especially in Fig. 12c, which means that the final manipulator end effector does not move precisely. Conversely, ADRC can make the end of the manipulator move into position with a small position error. This is because the feedback linearized PD is too sensitive to model parameter errors, and cannot compensate for unknown items such as hydrodynamic disturbances. The traditional PD control is unfit to the nonlinear system, making unsatisfactory control effect. Although CSMC is sensitive to disturbances and model errors, it is easy to generate high-frequency chattering on the sliding mode surface, which makes the instantaneous overshoot too large. The extended state observer in the ADRC method can compensate the internal disturbance caused by the model error and the system external disturbance caused by the external hydrodynamic term. Thereby, the better control accuracy and robustness against disturbances are realized by ADRC method.

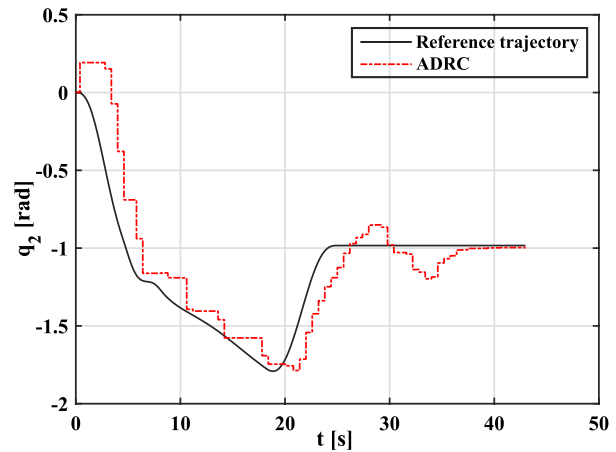
Comparing the root mean square error of these three controllers in Table 4, the proposed controller has the smallest comprehensive tracking control error during the entire cooperative grasping motion process of the underwater manipulator system.

7 Conclusion

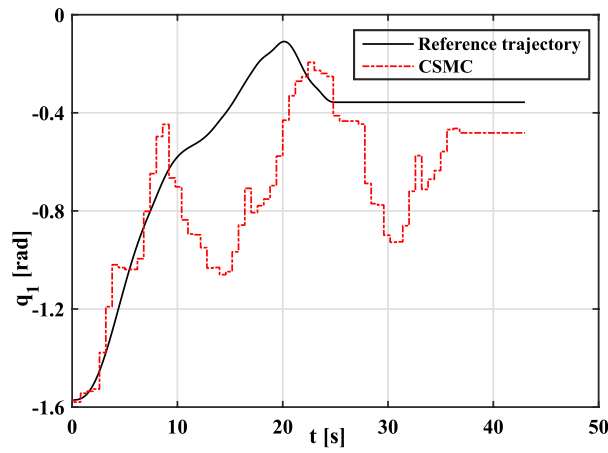
The robustness and disturbance rejection of an ADRC method to the uncertainties of an underwater manipulator has been studied. The ADRC concept was implemented and simulated on the two rotational joints of the concerned manipulator. The ADRC does not require accurate data of the manipulator but require inertial matrix M to decouple the static coupling part. For the purpose of the experiments, the control quality of ADRC in the presence of inertial matrix



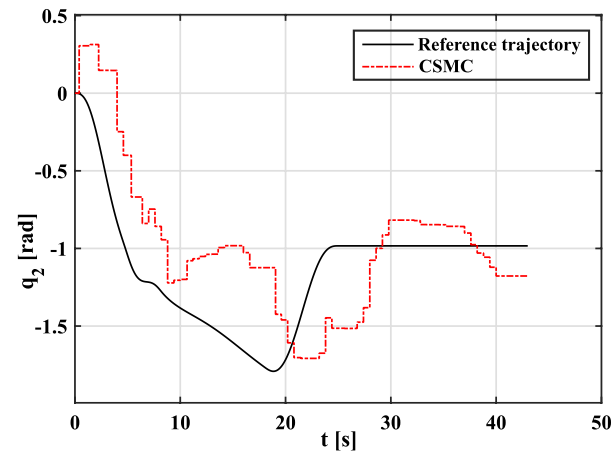
a First joint tracking trajectory using ADRC



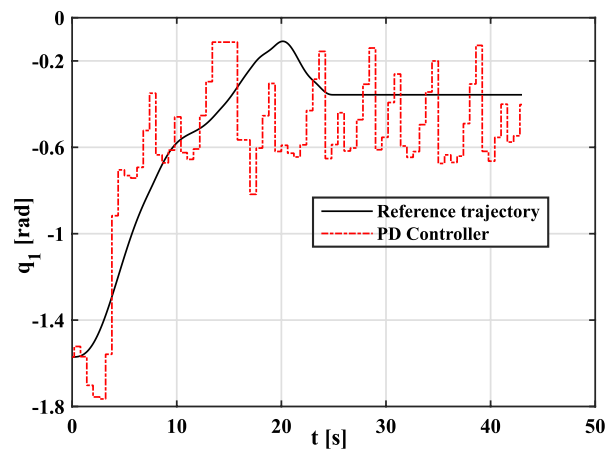
b Second joint tracking trajectory using ADRC



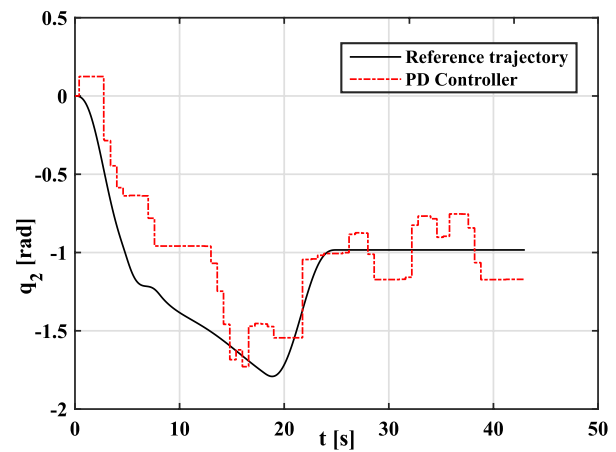
c First joint tracking trajectory using CSMC



d Second joint tracking trajectory using CSMC



e First joint tracking trajectory using PD



f Second joint tracking trajectory using PD

Fig. 12 Joint angle curves of trajectory tracking motion process of underwater manipulator under different controllers

Table 4 Root mean square error of trajectory tracking of each joint based on different controllers

Controller	link M_1 /rad	link M_2 /rad
ADRC	0.1401	0.2137
CSMC	0.3192	0.4110
Feedback linearized PD	0.2600	0.2724

errors was first adjusted and verified. Then, in the case of external disturbances on the manipulator, ADRC compares the quality of trajectory tracking control with traditional PD control and CSMC. Finally, based on the underwater manipulator hardware platform, the trajectory tracking control experiment was carried out.

The ADRC defines the internal disturbance and external fluid disturbance as the total disturbance, which is estimated and compensated by ESO. From the simulation results, ADRC has good robustness of control parameter. In the presence of inertial matrix errors, it can maintain better tracking quality although it has a certain impact on the transition process in the early stage of tracking. In the comprehensive comparisons with traditional PD control and CSMC in both simulation and experiment, the results illustrate the effectiveness of the proposed design and it is demonstrated that ADRC's control effect outperforms PD and CSMC in accuracy, dynamic characteristics and robustness.

Author Contributions All the authors have contributed to the concept and design of the research. Qirong Tang proposed the investigation originally and organized the work from the beginning to the end, while he also wrote and revised the texts with several rounds. Daopeng Jin developed the trajectory tracking control algorithm, implemented the source code, and prepared manuscript materials. During the research, Jiang Li and Minghao Liu built experimental framework, and executed the experiments. Rong Luo, Rui Tao, Chonglun Li, and Chuan Wang prepared simulation studies and data analysis, provided experiment occasions. The final manuscript was revised and approved by all authors.

Funding This work is supported by the project of National Natural Science Foundation of China (No. 62373285), the Innovative Projects (No. 2021-XXXX-LB-010-11), the Shanghai 2021 "Science and Technology Innovation Action Plan" with Special Project of Biomedical Science and Technology Support (No. 21S31902800), and the Key Pre-Research Project of the 14th-Five-Year-Plan on Common Technology. Meanwhile, this work is also partially supported by the Fundamental Research Funds for the Central Universities and the "National High Level Overseas Talent Plan" project, the "National Major Talent Plan" project (No. 2022-XXXX-XXX-079), as well as one key project (No. XM2023CX4013). It is also partially sponsored by the fundamental research project (No. XXXX2022YYC133), the Shanghai Industrial Collaborative Innovation Project (Industrial Development Category, No. HCXBCY-2022-051), Laboratory fund of Wuhan Digital Engineering Institute of CSSC, the project of Shanghai Key Laboratory of Spacecraft Mechanism (No. 18DZ2272200), as well as the project of Space Structure and Mechanism Technology Laboratory of China Aerospace Science and Technology Group Co. Ltd (No. YY-F805202210015). All these supports are highly appreciated.

Code or data availability It is not applicable and no extra data or material is available.

Declarations

Conflict of interest The authors declare that they have no conflicts of interest to this work.

Ethics approval This research does not involve human or animal subjects and does not require ethical approval.

Consent to participate This research does not involve human subjects and does not require consent to participate.

Consent for publication This research does not contain any individual person's data in any form (including any individual details, images or videos) and does not require consent for publication.

References

- Kozłowski K, Pazderski D, Krysiak B, Jedwabny T, Piasek J, Kozłowski S, Brock S, Janiszewski D, Nowopolski K (2020) High precision automated astronomical mount. In: Szewczyk R, Zieliński C, Kaliczyńska M (eds) Automation 2019, Springer, Cham, pp 299–315
- Ridgely DB, McFarland MB (1999) Tailoring theory to practice in tactical missile control. *IEEE Control Syst Mag* 19(6):49–55
- Wan C, Zhou H, Liu G (2020) Summary of control algorithm for underwater robot. In: the 5th international conference on mechanical, *Control Comput Eng (ICMCCE 2020)*, pp 759–762
- Lu D, Xiong C, Zeng Z, Lian L (2020) Adaptive dynamic surface control for a hybrid aerial underwater vehicle with parametric dynamics and uncertainties. *IEEE J Ocean Eng* 45(3):740–758
- Zhao S, Yuh J (2005) Experimental study on advanced underwater robot control. *IEEE Trans Robot* 21(4):695–703
- Wang L, Wang C, Du W, Meng Q (2005) Design of hydraulic control system for an underwater manipulator based on fuzzy-pid. *Chin Hydraul Pneum* 9(1):27–31
- Wang L, Wang C, Luo L, Yan H (2020) Research on feedforward compensation control strategy of electro-hydraulic servo system for underwater manipulator. *Control Inform Technol* 27(3):8–13
- Huang Q, Wang C, Liu X, Sun Z (2020) Research on adaptive control technology of underwater manipulator. *Mach Tool Hydraul* 38(24):80–82
- Wang S, Chen G, Wu L (2019) Neural network control with disturbance observer for uncertain robot manipulator. *J Comput* 14(1):71–78
- Zhu Q, Chen Y, Wang H (2009) The rbf neural network control for the uncertain robotic manipulator. In: 2009 international conference on machine learning and cybernetics, vol 3, pp 1266–1270
- Zhan Q, Zhang A (2006) Research on coordinated motion of an autonomous underwater vehicle-manipulator system. *Ocean Eng* 24(3):79–84
- Soylu S, Buckham BJ, Podhorodeski RP (2008) Development of a coordinated controller for underwater vehicle-manipulator systems. In: OCEANS 2008, pp 1–9
- Tomei P (1991) Adaptive pd controller for robot manipulators. *IEEE Trans Robot Autom* 7(4):565–570

14. Zhang W, Qi N, Yin H (2011) Neural network tracking control of space robot based on sliding mode variable structure. *Control Theory Appl* 28(9):1141–1144
15. Xu B, Pandian SR, Petry F (2005) A sliding mode fuzzy controller for underwater vehicle-manipulator systems. In: 2005 annual meeting of the North American fuzzy information processing society (NAFIPS 2005), pp 181–186
16. Han J (2009) From pid to active disturbance rejection control. *IEEE Trans Ind Electron* 56(3):900–906
17. Han J (2008) Active disturbance rejection control technique—the technique for estimating and compensating the uncertainties, 1st edn. National Defense Industry Press, Beijing, China
18. Han J (1995) Nonlinear states error feedback control law—nlsef. *Control Decis* 10(3):221–225
19. Przybyła M, Kordasz M, Madoński R, Herman P, Sauer P (2012) Active disturbance rejection control of a 2dof manipulator with significant modeling uncertainty. *Bull Polish Acad Sci* 60(3):509–520
20. Gao Z (2006) Active disturbance rejection control: a paradigm shift in feedback control system design. In: 2006 American control conference, p 7
21. Abdallah MAY, Fareh R (2019) Tracking control of serial robot manipulator using active disturbance rejection control. In: 2019 advances in science and engineering technology international conferences (ASET), pp 1–5
22. Patelski R, Dutkiewicz P (2020) On the stability of adrc for manipulators with modelling uncertainties. *ISA Trans* 102:295–303
23. Avila JPI, Adamowski JC (2011) Experimental evaluation of the hydrodynamic coefficients of a rov through morison's equation. *Ocean Eng* 38(17):2162–2170

Publisher's Note Springer Nature remains neutral with regard to jurisdictional claims in published maps and institutional affiliations.

Springer Nature or its licensor (e.g. a society or other partner) holds exclusive rights to this article under a publishing agreement with the author(s) or other rightsholder(s); author self-archiving of the accepted manuscript version of this article is solely governed by the terms of such publishing agreement and applicable law.